ISSN 1547-4771, Physics of Particles and Nuclei Letters, 2016, Vol. 13, No. 4, pp. 427–435. © Pleiades Publishing, Ltd., 2016.

PHYSICS OF ELEMENTARY PARTICLES AND ATOMIC NUCLEI. THEORY

Sub-Barrier Fusion Excitation Function Data and Energy Dependent Woods–Saxon Potential[1]

Manjeet Singh Gautam

Department of Physics, Indus Degree College, Kinana, Jind-126102, Haryana, India

e-mail: gautammanjeet@gmail.com

Received January 14, 2015

Abstract—This paper analyzed the role of intrinsic degrees of freedom of colliding nuclei in the enhancement of sub-barrier fusion cross-section data of various heavy ion fusion reactions. The influences of inelastic surface vibrations of colliding pairs are found to be dominant and their couplings result in the significantly larger fusion enhancement over the predictions of the one dimensional barrier penetration model at sub-barrier energies. The theoretical calculations are performed by using energy dependent Woods–Saxon potential model (EDWSP model) in conjunction with the one dimensional Wong formula. The effects of dominant intrinsic channels are entertained within framework of the coupled channel calculations obtained by using the code CCFULL. It is quite interesting to note that the energy dependence in Woods–Saxon potential simulates the effects of inelastic surface vibrational states of reactants wherein significantly larger value of diffuseness parameter ranging from $a = 0.85fm$ to $a = 0.95fm$ is required to address the observed fusion excitation function data of the various heavy ion fusion reactions.

DOI: 10.1134/S1547477116040063

1. INTRODUCTION

Dynamics of fusion reactions at near barrier and sub-barrier energies is an active area of research on the theoretical as well as on the experimental grounds. Heavy ion fusion reactions can be used to probe different aspects of nuclear interactions and nuclear structure of colliding nuclei. The importance of fusion reactions is also evident from production of nuclei away from the valley of stability and superheavy elements. During last few decades, an anomalously large enhancement in the sub-barrier fusion cross-sections in comparison to the predictions of one dimensional barrier penetration model, which have been observed in many projectile-target combinations, shows puzzling features of the low energy fusion excitation function data [1–7]. Such fusion enhancement of dinuclear system has an intimate link with the internal degrees of freedom of reactants such as permanent deformation, vibrations of nuclear surface, rotations, neck formation and nucleon transfer reactions. The relations between static deformation and inelastic surface vibrations with sub-barrier fusion enhancement have been well established by various coupled channel formulation and hence strongly recomanded that such internal structure degrees of freedom of fusing pairs can be ascribed for an anomalous behaviour of the fusion cross-section data in the domain of the Coulomb barrier [1–18].

The nucleus-nucleus potential, which is directly related with the fundamental characteristics of nuclear interactions, plays a central role in the good understanding of the nuclear reaction dynamics. The properties of surface region of nucleus-nucleus potential can be extracted by studying the elastic and inelastic scattering process while the properties of inner region of nucleus-nucleus potential can be explored by studying the fission and fusion reactions [19–21]. The Coulomb and centrifugal terms are well understood due to their simple expression whereas because of the large ambiguities in the optimum form of nuclear potential, it limits the complete understanding of nuclear reaction dynamics. Among different forms of nuclear potential proposed in literature, the standard energy independent Woods–Saxon potential is most widely used for description of the diverse form of nuclear interactions [22–29]. The various theoretical models also make the use of this potential for exploring the sub-barrier fusion dynamics [1–7]. A value of $a = 0.65fm$ is best suited for elastic scattering analysis. Interestingly, the diffuseness parameter of static Woods–Saxon potential is related to the slope of fusion excitation functions and significantly larger value of diffuseness parameter ranging from $a = 0.75fm$ to $a = 1.5fm$ has been exploited to explain the observed fusion dynamics. Surprisingly, the cause of this diffuseness anomaly, which might be an artifact of various kinds static and dynamical physical effects, is still far from good understanding [30, 31].

[1] The article is published in the original.

Following this concept, the present work is motivated to address the fusion dynamics of $^{16}_{8}O + ^{46,50}_{22}Ti$, $^{16}_{8}O + ^{58,60,64}_{28}Ni$ and $^{58}_{28}Ni + ^{58}_{28}Ni$ reactions within the context of the energy dependent Woods–Saxon potential model (EDWSP model) [32–47] and coupled channel approach [48]. In EDWSP model, closely similar physical effects that are induced because of couplings between elastic channel and internal structure degrees of freedom of fusing nuclei can be governed by introducing the energy dependence in the nucleus-nucleus real potential in such a way that it becomes more attractive at sub-barrier energies. The energy dependent nucleus-nucleus potential in conjunction with one dimensional Wong formula [49] predicts significantly larger sub-barrier fusion cross-sections with respect to the energy independent one dimensional barrier penetration model [32–47]. Very recently, the EDWSP model has been successfully used for entertaining the effects of neutron transfer channels and inelastic surface vibrations in the fusion dynamics of wide range of projectile-target combinations. The present work has been extended to explain effects of rapid variation of collectivity of target nuclei, target isotopic dependence of sub-barrier fusion enhancement and also explore the fusion hindrance at deep sub-barrier energies. In case of $^{16}_{8}O + ^{46,50}_{22}Ti$ and $^{16}_{8}O + ^{58,60,64}_{28}Ni$ reactions, the common projectile ($^{16}_{8}O$) is kept as inert while the low lying surface vibrational states of target nuclei are included in the coupled channel calculations performed by using the code CCFULL [48]. Various coupled channel models suggested that the fusion dynamics of $^{16}_{8}O + ^{46,50}_{22}Ti$, $^{16}_{8}O + ^{58,60,64}_{28}Ni$ and $^{58}_{28}Ni + ^{58}_{28}Ni$ systems are significantly influenced by the inelastic surface vibrational states such as $2^{+}$and 3^{-}vibrational states of target nuclei [50–52]. Furthermore, the applicability of the EDWSP model has also been tested for the exploration of the fusion dynamics of $^{58}_{28}Ni + ^{58}_{28}Ni$ reaction wherein the hindrance of the fusion excitation function data with respect to the coupled channel calculations has been clearly identified [52]. Therefore, due to the energy dependence in nucleus-nucleus potential, the EDWSP model calculation results in the barrier modification effects and hence adequately describes the observed sub-barrier fusion enhancement of various heavy ion fusion reactions. It is worth noting here that the energy dependence in nucleus-nucleus potential simulates the dominant effects of nuclear structure degrees of freedom of the fusing systems in the sub-barrier fusion dynamics. The details of the theoretical method adopted for this paper is discussed in section 2. The results are discussed in detail in section 3 while the summary of the work is presented in section 4.

2. THEORETICAL FORMALISM

2.1. One Dimensional Wong Formula

The partial wave fusion cross-section is given by the following expression

$$\sigma_F = \frac{\pi}{k^2}\sum_{\ell=0}^{\infty}(2\ell+1)T_\ell^F. \quad (1)$$

Hill and Wheeler proposed an expression for tunneling probability (T_ℓ^F) which is based upon the parabolic approximation wherein the effective interaction between the collision partners has been replaced by an inverted parabola [53]

$$T_\ell^{HW} = \frac{1}{1+\exp\left[\frac{2\pi}{\hbar\omega_\ell}(V_\ell - E)\right]}. \quad (2)$$

This approximation was further simplified by Wong using the following assumptions for barrier position, barrier curvature and barrier height [49].

$$R_\ell = R_{\ell=0} = R_B, \quad \omega_\ell = \omega_{\ell=0} = \omega$$

$$V_\ell = V_B + \frac{\hbar^2}{2\mu R_B^2}\left[\ell+\frac{1}{2}\right]^2.$$

By using these assumptions and Eq. (2) into Eq. (1), the fusion cross-section can be written as

$$\sigma_F = \frac{\pi}{k^2}\sum_{\ell=0}^{\infty}(2\ell+1)\frac{1}{1+\exp\frac{2\pi}{\hbar\omega}[V_\ell - E]}. \quad (3)$$

Wong assumes that the infinite number of partial waves contribute to the fusion process so one can change the summation over ℓ into integral with respect to ℓ in Eq. (3) and by solving the integral one can get the following expression of Wong formula [49].

$$\sigma_F = \frac{\hbar\omega R_B^2}{2E}\ell n\left[1+\exp\left(\frac{2\pi}{\hbar\omega}(E-V_B)\right)\right]. \quad (4)$$

2.2. Energy Dependent Woods–Saxon Potential Model (EDWSP Model)

Very recently, the EDWSP model has been successfully used to probe the role of nuclear structure of degrees of freedom of the colliding pairs on the dynamics of sub-barrier fusion cross-sections. The theoretical calculations make the use of the EDWSP model in conjunction with one dimensional Wong formula and static Woods–Saxon potential in the coupled channel calculations. Therefore, the shape of static Woods–Saxon potential is defined as

$$V_N(r) = \frac{-V_0}{\left[1+\exp\left(\frac{r-R_0}{a}\right)\right]} \quad (5)$$

with $R_0 = r_0(A_P^{1/3} + A_T^{1/3})$. The quantity V_0 is depth and a is diffuseness parameter of Woods–Saxon potential.

In EDWSP model, the depth of real part of Woods–Saxon potential is defined as

$$V_0 = \left[A_P^{2/3} + A_T^{2/3} - (A_P + A_T)^{2/3}\right] \times \left[2.38 + 6.8(1 + I_P + I_T)\frac{A_P^{1/3}A_T^{1/3}}{\left(A_P^{1/3} + A_T^{1/3}\right)}\right] MeV \quad (6)$$

where $I_P = \left(\frac{N_P - Z_P}{A_P}\right)$ and $I_T = \left(\frac{N_T - Z_T}{A_T}\right)$ are the isospin asymmetry of colliding systems. This parameterization of potential depth has been deduced by reproducing the fusion excitation function data of large number of fusion reactions ranging from $Z_PZ_T = 84$ to $Z_PZ_T = 1640$ [32–47]. In heavy ion collisions, the various static and dynamical physical effects occur in the tail region of nuclear potential which in turn modify the parameters of the nuclear potential. In heavy ion collisions, the fluctuation in the surface energy of colliding nuclei strongly depends upon the collective motion of all the nucleons inside the nucleus. The first term in the square bracket of Eq. (6) accommodates such kinds of the static and dynamical physical effects. In addition to this, the densities of collision partners in neck region also responsible for fluctuations of diffuseness parameter of static Woods–Saxon potential which in turn bring the requirement of abnormally large diffuseness parameter ranging from $a = 0.75fm$ to $a = 1.5fm$ for accounting the fusion excitation function data [1–7, 30, 31]. The second term inside the square bracket of Eq. (6) is directly proportional to isospin asymmetry effects of colliding nuclei which is different for different isotopes of a particular element. The isotopic effects of reactants are entered in the nucleus-nucleus potential through this term. Furthermore, the non-local quantum effects that arise due to the nucleon-nucleon interactions induce the energy dependence in nucleus-nucleus potential. The energy dependence in nucleus-nucleus potential is also reflected from the microscopic time dependent Hartree–Fock theory wherein it arises due to various channel coupling effects [54–57]. Therefore, owing to the importance of the fluctuations of diffuseness parameter of Woods–Saxon potential, the energy dependence in Woods–Saxon potential is taken via its diffuseness parameter. The energy dependent diffuseness parameter is defined as [32–47].

$$a(E) = 0.85\left[1 + \frac{r_0}{13.75\left(A_P^{-1/3} + A_T^{-1/3}\right)\left(1 + \exp\left(\frac{\frac{E}{V_{B0}} - 0.96}{0.03}\right)\right)}\right] fm. \quad (7)$$

In real physical situations, there is dissipation of kinetic energy of relative motion to internal structure of colliding pairs which must be incorporated in the theoretical calculations of the fusion excitation functions. Therefore, in fusion dynamics, the variation of surface energy, N/Z ratio, variation of densities in neck region, dissipation of kinetic energy of relative motion to internal structure of collision partners or other static and dynamical physical effects, which brings the modification in the value of diffuseness parameter of static Woods–Saxon potential, are accurately accommodated in the EDWSP model. In EDWSP model calculations; all such physical effects are entering through energy dependent diffuseness parameter [see Eq. (7)]. For heavy ion fusion reactions, the EDWSP model provides a wide range of diffuseness parameter depending upon the value of range parameter (r_0) and bombarding energy of reactants. The value of range parameter (r_0) is adjusted in order to vary the diffuseness parameter required to address the observed fusion excitation function data of fusing system under consideration [32–47]. It will be shown later that the theoretical calculations based upon static Woods–Saxon potential (CCFULL calculations) must include different kinds of channel coupling effects such as inelastic surface excitations of colliding pairs, rotational states of deformed nuclei and multi-nucleon transfer channels or other static and dynamical physical effects to reproduce the sub-barrier fusion data. However, the energy dependence in Woods–Saxon potential produces similar kinds of barrier modification effects that arise due to coupling of relative motion of reactants to their intrinsic degrees of freedom and thus accurately explain the energy dependence of sub-barrier fusion cross-section data.

2.3. Coupled Channel Model

This section briefly reviews the structure of the coupled channel model. Theoretically, the standard way to entertain the effects of internal structure degrees of freedom of colliding nuclei is to solve the coupled channel equations by including all the relevant channels [48, 58, 59]. Therefore, the set of the coupled channel equations can be written as

$$\left[\frac{-\hbar^2}{2\mu}\frac{d^2}{dr^2} + \frac{J(J+1)\hbar^2}{2\mu r^2} + V_N(r) + \frac{Z_PZ_Te^2}{r} + \varepsilon_n - E_{cm}\right] \times \psi_n(r) + \sum_m V_{nm}(r)\psi_m(r) = 0, \quad (8)$$

Table 1. The deformation parameter (β_λ) and the corresponding energy (E_λ) of the quadrupole and octupole vibrational states of various colliding nuclei

Nucleus	β_2	E_2, MeV	β_3	E_3, MeV	Reference
$^{16}_{8}$O	0.362	6.917	0.370	6.192	[60]
$^{46}_{22}$Ti	0.317	0.899	0.122	3.059	[12]
$^{50}_{22}$Ti	0.166	1.555	0.156	4.410	[12]
$^{58}_{28}$Ni	0.183	1.450	0.175	4.480	[61]
$^{60}_{28}$Ni	0.207	1.330	0.190	4.040	[61]
$^{64}_{28}$Ni	0.179	1.350	0.230	3.560	[61]

where, $\vec{r}$ is the radial coordinate for the relative motion between fusing nuclei. μ is defined as the reduced mass of the projectile and target system. The quantities E_{cm} and ε_n represent the bombarding energy in the centre of mass frame and the excitation energy of the n^{th} channel respectively. The V_{nm} is the matrix elements of the coupling Hamiltonian, which in the collective model consists of the Coulomb and nuclear components. For the coupled channel calculations, one can use the code CCFULL [48] wherein the coupled channel equations are numerically solved by using the following basic approximations. The rotating frame approximation has been used for reducing the number of the coupled channel equations [48, 58, 59]. In the condition of no transfer of the angular momentum from relative motion of reactants to their intrinsic motion, the total orbital angular momentum quantum number L can be replaced by the total angular momentum quantum number J. This approximation is also known as the isocentrifugal approximation. Under this approximation, the number of coupled channel equation reduced to great extent. For instance, in this approximation, the z-axis is chosen in the direction of the relative separation $\vec{r}$ of colliding nuclei so that $\theta = 0$ and the spherical harmonics become $Y^*_{\lambda\mu}(\hat{r}) = \sqrt{\frac{2\lambda+1}{4\pi}}\delta_{\mu,0}$. This implies that the excited states of each nucleus will have same spin projection on the rotating z-axis as in the respective ground states and the numbers of the coupled equations to be solved are significantly reduced. For example, the multipole excitation $0^+ \to \lambda$ is represented by only one channel in this approximation whereas $(\lambda + 1)$ channels are required in the full problem. Specifically, if one want to entertain 0^+, 2^+, $4^+$and 6^+ rotational states of the deformed nucleus a set of 16 coupled channel equations is to be solved but in rotating frame approximation, one has to solve only 4 coupled channel equations [48, 58, 59]. The ingoing wave boundary conditions (IWBC), which are well applicable for heavy ion reactions, are another approximations used to obtain the numerical solution of the coupled channel equations. According to IWBC, there are only incoming waves at the minimum position of the Coulomb pocket inside the barrier and there are only outgoing waves at infinity for all channels except the entrance channel ($n=0$) [48, 58, 59]. The code CCFULL [48] makes the use of static Woods–Saxon potential for addressing the role of the internal structure degrees of freedom of colliding pairs such as inelastic surface vibrations, rotational states and multi-nucleon transfer channels. By including all the relevant channels, the fusion cross-section can be written as

$$\sigma_F(E) = \sum_J \sigma_J(E) = \frac{\pi}{k_0^2}\sum_J (2J+1)\,P_J(E) \qquad (9)$$

where, $P_J(E)$ is the total transmission coefficient corresponding to the angular momentum J.

3. RESULTS AND DISCUSSION

The focus of the present work is to address the interplay of the vibrational states of colliding systems on the energy dependence of the fusion excitation functions at sub-barrier energies. The inclusions of these collective vibrational states significantly enhance the magnitude of sub-barrier fusion cross-sections over the predictions of the one dimensional barrier penetration model. Furthermore, the effects of rapid variation of collectivity of target nuclei as well as the target isotopic dependence of the sub-barrier fusion enhancement are also evident from the analysis of $^{16}_{8}\mathrm{O} + {}^{46,50}_{22}\mathrm{Ti}$, $^{16}_{8}\mathrm{O} + {}^{58,60,64}_{28}\mathrm{Ni}$ and $^{58}_{28}\mathrm{Ni} + {}^{58}_{28}\mathrm{Ni}$ reactions. The values of the deformation parameters and corresponding excitation energies of the low lying 2^+ and 3^- vibrational states of the colliding nuclei are listed in Table 1. The barrier height, barrier position and barrier curvature of the fusing nuclei as required in the EDWSP model calculations along with the one dimensional Wong formula is listed in Table 2. The values of range, depth and diffuseness parameters used in the EDWSP model calculations for various combinations of the colliding nuclei are listed in Table 3.

The spherical nuclei exhibit low lying inelastic surface vibrations as dominant mode of couplings and coupling to inelastic surface vibrations of colliding nuclei significantly enhances the magnitude of sub-barrier fusion cross-sections. The dynamics of spherical nuclei is expected to be very simple due to involvement of the fewer internal structure degrees of freedom and hence provides the concrete conclusion about the role played by the nuclear structure of reactants [50, 51]. In addition, the rapid variation of collectivity of target isotopes as well as the target isotopic dependence of the enhancement of sub-barrier fusion

cross-sections is directly reflected from the present analysis. As far as the projectile ($^{16}_{8}$O) is concerned, it possesses low lying surface vibrations only and due to very high excitation energies of the inelastic surface excitations, it offers negligible influence on the fusion dynamics of $^{16}_{8}O + {}^{46,50}_{22}Ti$ and $^{16}_{8}O + {}^{58,60,64}_{28}Ni$ systems [50, 51]. However, there is significant variation in the collectivity of 2^+vibrational states in target isotopes which mirrors the difference in the energy dependence of sub-barrier fusion cross-sections of these systems. The beauty of Ti-isotopes is that the collectivity decreases with increase of neutron richness and hence spans a significant variation in the quadrupole deformation with increase in the number of neutrons. Furthermore, due to low excitation energy ($E = 0.889$ MeV) and large qudruploe deformation of $^{46}_{22}$Ti nucleus, it exhibits the strongest low lying quadrupole vibration in the mass region $A = 40$–60. Therefore, the effects of the quadrupole vibrational states are more pronounced in comparison to that of the other vibrational states of the colliding pairs. As the strength of quadrupole deformation in $^{46}_{22}$Ti is almost double ($\beta_2 = 0.317$ and $E_2 = 0.889$ MeV) and lies at very small excitation energy with respect to the corresponding values in $^{50}_{22}$Ti ($\beta_2 = 0.166$ and $E_2 = 1.555$ MeV). Therefore, it is expected that the addition of the 2^+ vibrational state of $^{46}_{22}$Ti nucleus strongly alters the behavior of the low energy fusion excitation functions.

The octupole vibration in lighter target nucleus lies at low excitation energy in comparison to heavier target nucleus but has almost same coupling strength and hence displays weak influences on sub-barrier fusion process. For $^{16}_{8}O + {}^{46,50}_{22}Ti$ reactions, the experimental data are strongly under-predicted by the no coupling calculations wherein the colliding pairs are taken as inert. This suggests that the low lying surface vibrations of colliding nuclei must be incorporated to reproduce the sub-barrier fusion enhancement. The inclusion of one phonon 2^+ vibrational state of target alone or one phonon 3^- vibrational state of target alone unable to bring the observed fusion enhancement at below barrier energies. However, coupling to one phonon 2^+ and 3^- vibrational states along with their mutual couplings in target recover observed enhancement of sub-barrier fusion excitation function of $^{16}_{8}O + {}^{46,50}_{22}Ti$ reactions. The larger fusion enhancement of $^{16}_{8}O + {}^{46}_{22}Ti$ system (Fig. 1a) with respect to $^{16}_{8}O + {}^{50}_{22}Ti$ system (Fig. 1b) is the signature of the opposite target mass dependence of the sub-barrier fusion enhancement. In both cases, the possibility of the neutron transfer channel can be ruled out because of negative Q-values for neutron transfer channels.

Table 2. The values of V_{B0}, R_B and $\hbar\omega$ used in the EDWSP model calculations for various heavy ion systems

System	V_{B0}, MeV	R_B, fm	$\hbar\omega$, MeV	Reference
$^{16}_{8}O + {}^{46}_{22}Ti$	25.70	8.63	2.60	[50]
$^{16}_{8}O + {}^{50}_{22}Ti$	25.40	9.15	3.80	[50]
$^{16}_{8}O + {}^{58}_{28}Ni$	33.60	8.70	3.51	[51]
$^{16}_{8}O + {}^{60}_{28}Ni$	33.70	8.67	3.51	[51]
$^{16}_{8}O + {}^{64}_{28}Ni$	33.40	8.76	3.47	[51]
$^{58}_{28}Ni + {}^{58}_{28}Ni$	97.87	10.50	3.30	[48]

Table 3. Range, depth, diffuseness of Woods-Saxon potential used in EDWSP model calculations for various heavy ion fusion reactions [32–47]

System	r_0, fm	V_0, MeV	$\frac{a^{Present}}{Energy\ Range}$, $\frac{\text{fm}}{\text{MeV}}$
$^{16}_{8}O + {}^{46}_{22}Ti$	1.090	45.36	$\frac{0.94\ \text{to}\ 0.85}{15\ \text{to}\ 55}$
$^{16}_{8}O + {}^{50}_{22}Ti$	1.070	49.45	$\frac{0.94\ \text{to}\ 0.85}{15\ \text{to}\ 55}$
$^{16}_{8}O + {}^{58}_{28}Ni$	1.020	48.62	$\frac{0.94\ \text{to}\ 0.85}{25\ \text{to}\ 55}$
$^{16}_{8}O + {}^{60}_{28}Ni$	1.030	50.40	$\frac{0.94\ \text{to}\ 0.85}{25\ \text{to}\ 55}$
$^{16}_{8}O + {}^{64}_{28}Ni$	1.030	53.74	$\frac{0.94\ \text{to}\ 0.85}{25\ \text{to}\ 60}$
$^{58}_{28}Ni + {}^{58}_{28}Ni$	1.120	101.69	$\frac{0.95\ \text{to}\ 0.85}{90\ \text{to}\ 115}$

Therefore, the observed sub-barrier fusion enhancement can only be correlated with the dominance of the inelastic surface vibrations of target nuclei. It is worth mentioning here that the predictions of the EDWSP model along with the one dimensional Wong formula provide quite close agreement with the experimental data of $^{16}_{8}O + {}^{46,50}_{22}Ti$ reactions in all range of energies spread across the Coulomb barrier as evident from Fig. 1. The close resemblance of the predictions of the coupled channel model and the EDWSP model for

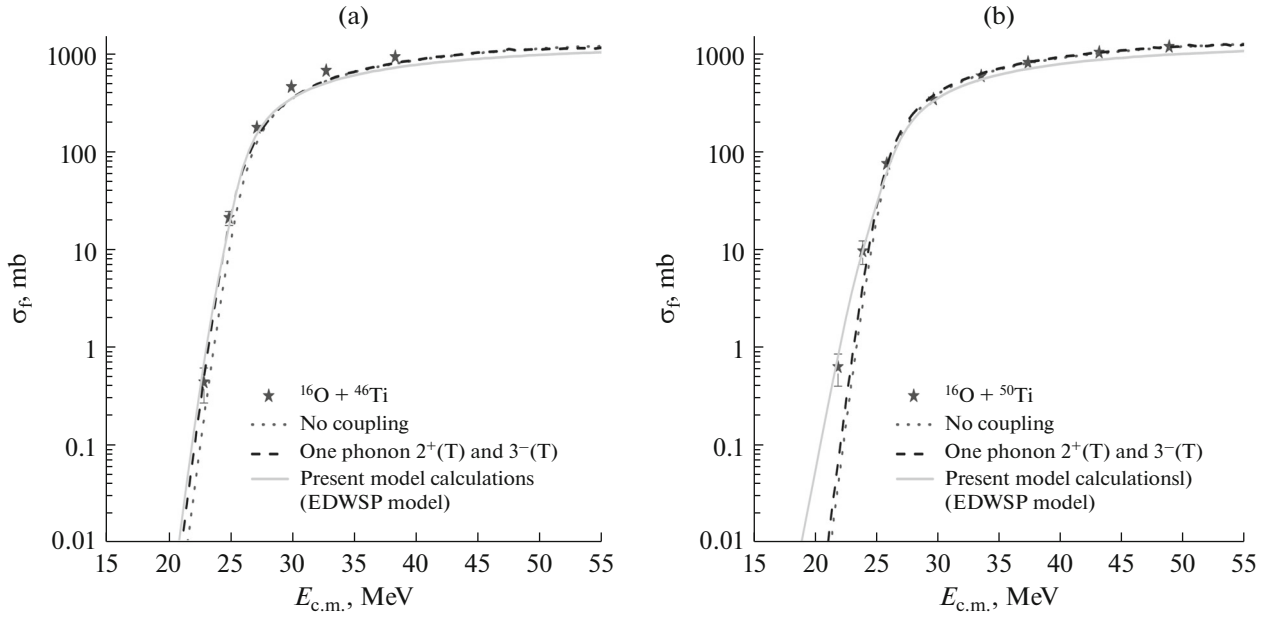

Fig. 1. The fusion excitation functions of $^{16}_{8}O + ^{46,50}_{22}Ti$ reactions obtained by using the EDWSP model [32–47] and coupled channel code CCFULL [48]. The theoretical results are compared with the available experimental data taken from Ref. [50].

observed fusion dynamics of $^{16}_{8}O + ^{46,50}_{22}Ti$ systems unambiguously indicates that the energy dependence in Woods–Saxon potential mimics the effects of dominant internal degrees of freedom of the collision partners.

The fusion dynamics of $^{16}_{8}O + ^{58,60,64}_{28}Ni$ systems [51] has been strongly influenced by the low lying surface vibrations of the Ni-isotopes and also display the target isotopic dependence of sub-barrier fusion enhancement. With the increase of neutron richness of target nuclei, the magnitude of the sub-barrier fusion enhancement increases and such physical effect in the fusion process is the consequence of different collective properties of Ni-isotopes. In other words, one can say that with increase of neutron richness in Ni-isotopes, the target nuclei become more collective and display its signature by enhancing the magnitude of sub-barrier fusion excitation function data. In this regard, the fusion dynamics of $^{16}_{8}O + ^{58,60,64}_{28}Ni$ systems is very interesting wherein with increase of the target isotopic mass, the excitation energies of inelastic surface vibrations decrease. Therefore, the effect of coupling of 2^+ and 3^- vibrational states in target nuclei becomes more pronounced as one move from the lighter target isotope to heavier target isotope and consequently, large isotopic enhancement in the fusion cross-sections has been found in sub-barrier energy regions. Due to the lower quadrupole excitation energy, the effect of coupling to 2^+ vibrational state of target is playing a significant role and hence strongly modifies the energy dependence of the sub-barrier fusion cross-sections of these fusing systems.

For $^{16}_{8}O + ^{58,60,64}_{28}Ni$ reactions, the projectile is taken as inert in the coupled channel calculations. If both colliding pairs are considered as inert, no coupling calculations are significantly smaller than that of the experimental fusion data. The inclusion of the single phonon 2^+ vibrational state alone in target or single phonon 3^- vibrational states alone in target fails to recover experimental fusion data particularly at below barrier energies. This suggested that more intrinsic channels are required to reproduce the observed fusion enhancement at sub-barrier energies. The couplings to one phonon 2^+ and 3^- vibrational states along with their mutual couplings in target reasonably account the magnitude of sub-barrier fusion enhancement for all Ni-isotopes. In the fusion of $^{16}_{8}O + ^{58,60,64}_{28}Ni$ systems, the coupled channel calculations show that the contribution of the inelastic surface vibrations enhances the sub-barrier fusion excitation functions over the predictions of the one dimensional barrier penetration model as evident from Fig. 2. Furthermore, it is worth noting here that the predictions made by the EDWSP model along with the one dimensional Wong formula give quite close agreement with the experimental data in domain of the Coulomb barrier. As both coupled channel model and the EDWSP model predict closely similar behavior of the various heavy ion fusion reactions which in turn concrete the conclusion that the EDWSP model mocks

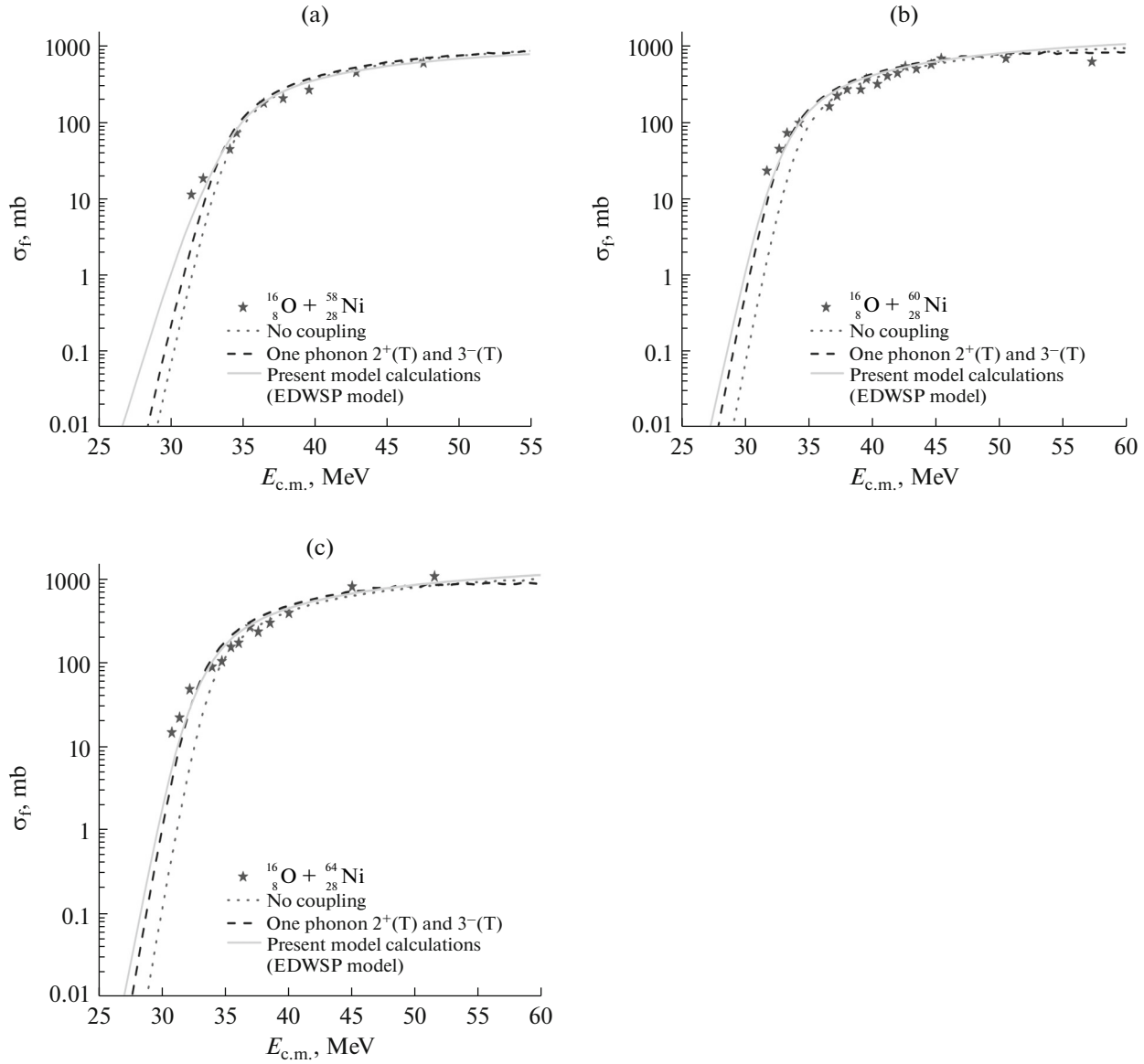

Fig. 2. Same as Fig. 1 but for $^{16}_{8}O + ^{58,60,64}_{28}Ni$ reactions. The theoretical results are also compared with the available experimental data taken from Ref. [51].

up the effects of dominant internal degrees of freedom of collision partners and hence produces barrier modification effects in similar way to that of the coupled channel approach.

It is quite interesting to check out the applicability of the EDWSP model to explain the observed fusion dynamics of $^{58}_{28}Ni + ^{58}_{28}Ni$ reaction. This reaction is chosen because of two reasons. The first reason is that the colliding pairs form a symmetric pair in the entrance channel and second reason lying in the interest to explore the fusion data particularly at deep sub-barrier energies. In literature, it has been well established that the fusion excitation function data of $^{58}_{28}Ni + ^{58}_{28}Ni$ reaction falls more steeply than the theoretical predictions of the coupled channel approach. This steep fall of the fusion excitation function data at deep sub-barrier energies is termed as fusion hindrance. For $^{58}_{28}Ni + ^{58}_{28}Ni$ reaction, the inelastic surface excitations such as one phonon, two phonon vibrational states are the dominant mode of couplings and the inclusion of such dominant collective vibrational states of the fusing pairs reasonably explain the observed fusion dynamics of chosen reaction in near and sub-barrier energy regions. However, at deep sub-barrier energies, such coupled channel calculations falls more slowly with reference to the experimentally observed fusion data. On the other hand, the energy dependence in nucleus-nucleus potential modifies the

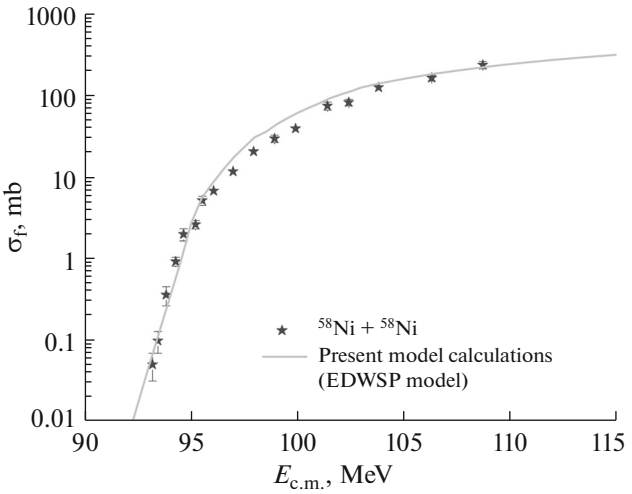

Fig. 3. Same as Fig. 1 but for $^{58}_{28}\mathrm{Ni} + ^{58}_{28}\mathrm{Ni}$ reaction. The theoretical results are also compared with the available experimental data taken from Ref. [52].

interaction barrier between the fusing pairs and adequately explains the observed fusion dynamics of $^{58}_{28}\mathrm{Ni} + ^{58}_{28}\mathrm{Ni}$ reaction in whole range of energy as shown in Fig. 3. This clearly reveals that the energy dependence in nucleus-nucleus potential introduces similar kinds of the barrier modification effects as observed in the usual coupled channel approach.

In literature, it is well recognized that the effect of couplings to inelastic excitations of projectile (target) or permanent deformations or nucleon (multi-nucleon) transfer is to split the Coulomb barrier into number of barriers of different heights which is known as barrier distribution. The penetration through the barriers whose height is smaller than that of the Coulomb barrier is more probable and hence ultimately predict large fusion enhancement at sub-barrier energies. Similarly, an energy dependent Woods–Saxon potential model (EDWSP model) produces a distribution of the energy dependent fusion barriers of varying height which is analogous to the distribution of barriers that arise due to various channel coupling effects and hence reasonably explains the dynamics of the various heavy ion fusion reactions. Therefore, the clarifications of the fact that the various kinds of static and dynamical physical effects that are induced due to intrinsic degrees of freedom such as inelastic surface vibrations, nucleon transfer channel and other dynamical effects whether represents a true picture of the dominant channels in sub-barrier fusion enhancement or simply mirror the limitations of the static Woods–Saxon potential parameters require more intensive studies. Furthermore, the energy dependence in Woods–Saxon potential whether represents optimum form of the nuclear potential or simulates other static and dynamical physical effects is still not clear.

4. CONCLUSIONS

This work analyzed the fusion dynamics of $^{16}_{8}\mathrm{O} + ^{46,50}_{22}\mathrm{Ti}$, $^{16}_{8}\mathrm{O} + ^{58,60,64}_{28}\mathrm{Ni}$ and $^{58}_{28}\mathrm{Ni} + ^{58}_{28}\mathrm{Ni}$ reactions in the close vicinity of the Coulomb barrier by using EDWSP model and coupled channel model. The role of inelastic surface vibrations such as 2^+ and 3^- vibrational states is entertained within the context of coupled channel calculations performed by using the code CCFULL. The coupled channel model and the EDWSP model provide closely similar behavior of the various heavy ion fusion reactions considered in the present work. This unambiguously mirrors that the energy dependence in Woods–Saxon potential introduces barrier modification effects in somewhat similar way to that of the usual coupled channel formulations and hence simulates different kinds of static and dynamical physical effects that arise because of coupling between relative motion of the fusing nuclei and their intrinsic degrees of freedom. Furthermore, significantly large values of diffuseness parameter ranging from $a = 0.85fm$ to $a = 0.95fm$ are necessarily required to bring the observed fusion enhancement at below barrier energies. This suggested that the EDWSP model has an effect that is closely similar to that of the static Woods–Saxon potential with abnormally large diffuseness parameter ranging from $a = 0.75fm$ to $a = 1.5fm$.

ACKNOWLEDGMENTS

This work has been supported by Dr. D.S. Kothari Post-Doctoral Fellowship Scheme sponsored by University Grants Commission (UGC), New Delhi, India.

REFERENCES

1. M. Beckerman, Rep. Prog. Phys. **51**, 1047 (1988).
2. W. Reisdorf, J. Phys. G **20**, 1297 (1994).
3. M. Dasgupta, D. J. Hinde, N. Rowley, and A. M. Stefanini, Ann. Rev. Nucl. Part. Sci. **48**, 401 (1998).
4. A. B. Balantekin and N. Takigawa, Rev. Mod. Phys. **70**, 77 (1998).
5. L. F. Canto, P. R. S. Gomes, R. Donangelo, and M. S. Hussein, Phys. Rep. **424**, 1 (2006).
6. K. Hagino and N. Takigawa, Prog. Theor. Phys. **128**, 1061 (2012).
7. B. B. Back, H. Esbensen, C. L. Jiang, and K. E. Rehm, Rev. Mod. Phys. **86**, 317 (2014).
8. H. Timmers, D. Ackermann, S. Beghini, L. Corradi, J. H. He, G. Montagnoli, F. Scarlassara, A. M. Stefanini, and N. Rowley, Nucl. Phys. A **633**, 421 (1998).
9. M. Trotta, A. M. Stefanini, L. Corradi, A. Gadea, F. Scarlassara, S. Beghini, and G. Montagnoli, Phys. Rev. C **65**, 011601 (2001).
10. A. M. Stefanini, B. R. Behera, S. Beghini, L. Corradi, E. Fioretto, A. Gadea, G. Montagnoli, N. Rowley, F. Scarlassara, S. Szilner, and M. Trotta, Phys. Rev. C **76**, 014610 (2007).

11. J. R. Leigh, M. Dasgupta, D. J. Hinde, J. C. Mein, C. R. Morton, R. C. Lemmon, J. P. Lestone, J. O. Newton, H. Timmers, J. X. Wei, and N. Rowley, Phys. Rev. C **52**, 3151 (1995).
12. A. A. Sonzogni, J. D. Bierman, M. P. Kelly, J. P. Lestone, J. F. Liang, and R. Vandenbosch, Phys. Rev. C **57**, 722 (1998).
13. H. M. Jia, C. J. Lin, F. Yang, X. X. Xu, H. Q. Zhang, Z. H. Liu, Z. D. Wu, L. Yang, N. R. Ma, P. F. Bao, and L. J. Sun, Phys. Rev. C **89**, 064605 (2014).
14. N. V. S. V. Prasad, A. M. Vinodkumar, A. K. Sinha, K. M. Varier, D. L. Sastry, N. Madhavan, R. Sugathan, D. O. Kataria, and J. J. Das, Nucl. Phys. A **603**, 176 (1996).
15. V. I. Zagrebaev, Phys. Rev. C **67**, 061601 (2003).
16. H. Q. Zhang, C. J. Lin, F. Yang, H. M. Jia, X. X. Xu, Z. D. Wu, F. Jia, S. T. Zhang, Z. H. Liu, A. Richard, and C. Beck, Phys. Rev. C **82**, 054609 (2010).
17. J. O. Newton, C. R. Morton, M. Dasgupta, J. R. Leigh, J. C. Mein, D. J. Hinde, and H. Timmers, Phys. Rev. C **64**, 064608 (2001).
18. A. M. Stefanini, G. Montagnoli, H. Esbensen, L. Corradi, S. Courtin, E. Fioretto, A. Goasduff, J. Grebosz, F. Haas, M. Mazzocco, C. Michelagnoli, T. Mijatovic, D. Montanari, G. Pasqualato, C. Parascandolo, et al., Phys. Lett. B **728**, 639 (2014).
19. W. D. Myers and W. J. Swaitecki, Phys. Rev. C **62**, 044610 (2000).
20. C. H. Dasso and G. Pollarolo, Phys. Rev. C **68**, 054604 (2003).
21. K. Hagino, N. Rowley, and M. Dasgupta, Phys. Rev. C **67**, 054603 (2003).
22. R. N. Sagaidak, S. P. Tretyakova, S. V. Khlebnikov, A. A. Ogloblin, N. Rowley, and W. H. Trzaska, Phys. Rev. C **76**, 034605 (2007).
23. N. Wang and W. Scheid, Phys. Rev. C **78**, 014607 (2008).
24. L. C. Vaz, Comput. Phys. Commun. **22**, 451 (1981).
25. V. V. Sargsyan, G. G. Adamian, N. V. Antonenko, and W. Scheid, Eur. Phys. J. A **45**, 125 (2010).
26. D. Sukhvinder, M. Singh, R. Kharab, and H. C. Sharma, Mod. Phys. Lett. A **26**, 1017 (2011).
27. D. Sukhvinder, M. Singh, and R. Kharab, Int. J. Mod. Phys. E **21**, 1250054 (2012).
28. D. Sukhvinder, M. Singh, R. Kharab, and H. C. Sharma, Commun. Theor. Phys. **55**, 649 (2011).
29. D. Sukhvinder, M. Singh, R. Kharab, and H. C. Sharma, Phys. At. Nucl. **74**, 49 (2011).
30. J. O. Newton, J. O. Newton, R. D. Butt, M. Dasgupta, D. J. Hinde, I. I. Gontchar, and K. Hagino, Phys. Rev. C **70**, 024605 (2004).
31. A. Mukherjee, D. J. Hinde, M. Dasgupta, K. Hagino, J. O. Newton, and R. D. Butt, Phys. Rev. C **75**, 044608 (2007).
32. M. Singh, D. Sukhvinder, and R. Kharab, Mod. Phys. Lett. A **26**, 2129 (2011).
33. M. Singh, D. Sukhvinder, and R. Kharab, Nucl. Phys. A **897**, 179 (2013).
34. M. Singh, D. Sukhvinder, and R. Kharab, Nucl. Phys. A **897**, 198 (2013).
35. M. Singh, D. Sukhvinder, and R. Kharab, AIP Conf. Proc. **1524**, 163 (2013).
36. M. Singh and R. Kharab, EPJ Web Conf. **66**, 03043 (2014).
37. M. Singh, Sukhvinder, and R. Kharab, Atti Della "Fondazione Giorgio Ronchi," Anno LXV **6**, 751 (2010).
38. M. Singh, M. Phil. Dissertation (Kurukshetra Univ., Kurukshetra, Haryana, India, 2009, unpublished).
39. M. Singh, PhD Thesis (Kurukshetra Univ., Kurukshetra, Haryana, India, 2013, unpublished).
40. M. S. Gautam, Phys. Rev. C **90**, 024620 (2014).
41. M. S. Gautam, Nucl. Phys. A **933**, 272 (2015).
42. M. S. Gautam, Mod. Phys. Lett. A **30**, 1550013 (2015).
43. M. S. Gautam, Phys. Scr. **90,** 025301 (2015).
44. M. S. Gautam, Phys. Scr. **90**, 055301 (2015), Phys. Scr. **90**, 125301 (2015), Indian J. Phys. **90**, 335 (2016) Braz. J. Phys. **46**, 143 (2016), Pramana **86**, 1067 (2016), Chinese Phys. C **40**, 054101 (2016), Chinese J. Phys. **54**, 86 (2016).
45. M. S. Gautam, Acta Phys. Polon. B **46**, 1055 (2015).
46. M. S. Gautam, Can. J. Phys. **93**, 1343 (2015), Chin. Phys. C **39**, 114102 (2015), Commun. Theor. Phys. **64**, 710 (2015).
47. M. S. Gautam, Kaur Amandeep, and M. K. Sharma, Phys. Rev. C **92**, 054605 (2015), M. S. Gautam and M. K. Sharma, AIP Conf. Proc. **1675**, 020052 (2015), M. S. Gautam, Rajni and M. K. Sharma, Braz. J. Phys. **46**, 133 (2016).
48. K. Hagino, N. Rowley, and A. T. Kruppa, Comput. Phys. Commun. **123**, 143 (1999).
49. C. Y. Wong, Phys. Rev. Lett. **31**, 766 (1973).
50. Neto R. Liguori, J. C. Acquadro, P. R. S. Gomes, A. S. de Toledo, C. F. Tenreiro, E. Crema, N. C. Filjo, and M. M. Coimnra, Nucl. Phys. A **512**, 333 (1990).
51. C. P. Silva, D. Pereira, L. C. Chamon, E. S. Rossi, Jr., G. Ramirez, A. M. Borges, and C. E. Aguiar, Phys. Rev. C **55**, 3155 (1997).
52. M. Beckerman, M. Salomaa, A. Sperduto, J. D. Molitoris, and A. di Rienzo, Phys. Rev. C **25**, 837 (1982).
53. D. L. Hill and J. A. Wheeler, Phys. Rev. **89**, 1102 (1953).
54. L. C. Chamon, B. V. Carlson, L. R. Gasques, D. Pereira, C. de Conti, M. A. G. Alvarez, M. S. Hussein, M. A. Cndido Ribeiro, E. S. Rossi, Jr., and C. P. Silva, Phys. Rev. C **66**, 014610 (2002).
55. K. Washiyama and D. Lacroix, Phys. Rev. C **74**, 024610 (2008).
56. C. Simenel, M. Dasgupta, D. J. Hinde, and E. Williams, Phys. Rev. C **88**, 064604 (2013).
57. A. S. Umar, C. Simenel, and V. E. Oberacker, Phys. Rev. C **89**, 034611 (2014).
58. H. Esbensen, S. Landowne, and C. Price, Phys. Rev. C **36**, 1216 (1987).
59. T. Rumin, K. Hagino, and N. Takigawa, Phys. Rev. C **61**, 014605 (1999).
60. V. Tripathi, T. Baby Lagy, J. J. Das, P. Sugathan, N. Madhavan, A. K. Sinha, P. V. Madhusudhana Rao, S. K. Hui, R. Singh, and K. Hagino, Phys. Rev. C **65**, 014614 (2001).
61. A. M. Vinodkumar, K. M. Varier, N. V. S. V. Prasad, D. L. Sastry, A. K. Sinha, N. Madhavan, P. Sugathan, D. O. Kataria, and J. J. Das, Phys. Rev. C **53**, 803 (1996).